Mansoura Engineering Journal

Volume 20 | Issue 1 Article 3

3-1-2020

Thermal Behaviour Topological Analysis of High Starting Torque Squirrel Cage Rotor Winding.

M. El-Shamoty
Electrical Power and Machine Department Engineering, Faculty of Engineering, El-Mansoura University, Mansoura, Egypt.

THERMAL BEHAVIOUR TOPOLOGICAL ANALYSIS OF HIGH STARTING TORQUE SQUIRREL CAGE ROTOR WINDING

"التحليل الطوبوجرافي للسلوك الحراري لملف العضو الدوار ذو قفص السنجاب عالي عزم بدء الحركه"

By
M.M.I. EL-SHAMOTY

DEPARTMENT OF ELECTRICAL POWER AND MACHINE, FACULTY OF ENGINEERING, MANSOURA UNIVERSITY, EL-MANSOURA, EGYPT.

الخلاصة : ان حساب السلوك الحراري في موصلات قفص السنجاب المستخدمة في بناء المحركات الاستنتاجية ذات عزم بدء الحركه العالي خطوه من اهم خطوات تصميم تلك الآلة ، حيث يتوقف اعتماد التصميم المقترح أو تعديله علي نتائج تلك الخطوة بهدف الوصول الي بناء محرك متين يمكنه مواجهة ظروف التشغيل غير العادية .

يقدم البحث "نموذجا رياضيا" علي درجه ملحوظه من الدقه يمكن استخدامه بسهولة في حساب السلوك الحراري في الموصلات العميقة المستخدمة في بناء العضو الدوار بالمحركات المذكورة تحت ظروف تشغيل مختلفة. وتقوم فكره النموذج علي استخدام "شبكة حرارية مكافئة" يتم بواسطتها تمثيل عمليات انتقال الحراره خلال "النموذج التكراري" للموصل في الظروف العابرة والمستقرة . يتوقف عدد المعادلات التفاضلية الناشئة ، وبالتالي عدد النقاط في اتجاه عمق الموصل التي يمكن عندها متابعة السلوك الحراري ، علي عدد "القطاعات الجزئية الوهمية" التي يتم تقسيم قطاع الموصل اليها . لذا فإنه من السمات المهمة للنموذج الرياضي المقترح هو إمكانية اقامة تلك المعادلات باستخدام "التحليل الطوبوجرافي للشبكات" ، مهما كان عدد نقاط المتابعة ، بمساعدة "خوارزم منطقي" تم برمجته للحاسب الالي . كما ان النموذج يأخذ في الاعتبار تأثير "الظاهرة القشرية" علي تيار الموصل وايضا تأثير الحرارة علي كل من كثافة التيار ومقاومة الموصل .

وقد تم وضع "برنامج للحاسب الآلي" يحاكي النموذج الرياضي المقترح متضمنا برامج جزئية للعمليات المنطقية اللازمة للبناء الذاتي للشبكة الحرارية المكافئة طبقا لعدد نقاط المتابعة ، والبناء الذاتي طوبوجرافيا للمعادلات اللازمة ،وإعداد "القيم الأولية اللحظية" علي كل من الجانب الحراري والكهربي للمشكلة واللازمة اثناء اجراء الحل . والبرنامج قابل للدمج والتكامل مع برامج التصميم الخاصة بالآلة المذكورة.

ويقوم البرنامج بحساب السلوك الحراري عند نقاط المتابعة ، والتي لايجب ان تقل عن سبعة لدقة المحاكاة وايضا "توزيع درجات الحرارة "في اتجاه عمق الموصل اثناء بدء الحركة حتي السرعه المستقرة وايضا في ظروف تشغيل مغايرة مثل بدء الحركه التكراري بدون توقف لدورات تحميل مختلفة.

ويقترح الباحث انة بتحليل النتائج المحسوبة لعديد من المحركات ذات القدرات وظروف التشغيل المختلفة باستخدام هذا البرنامج تنشأ "قاعده اساسية للمعلومات" تساعد في اتخاذ القرارات الخاصة بشكل الموصل ، وحدود التشغيل الآمن، والبيانات الحرارية الخاصة بنظم الحمايه .

ABSTRACT :

In design of high starting torque squirrel cage induction motors a proper estimation of the cage winding thermal behaviour under different operating conditions must be carried out. This estimation is an essential step of motor

design. According to its results the design scheme can be approved or modified to ensure the building of a reliable motor.

This peper presents a mathematical model that calculates the thermal behaviour of wedge-type rotors under different operating conditions. The model is based on the concept of building an equivalent thermal network of the bar. The number of lumped thermal meshes, and in turn the number of required differential equations, depends on the number of fictitious sub-sections into which the bar cross-sectional area is divided. The model considers skin effect during the starting period as well as the temperature effect on the current density distribution and the bar resistance. Further more, the proposed model has the ability of applying the topological network analysis.
Therefore, and regardless of the number of subsections, the process of building the required equation system can be carried out by a relevant computer routine.

The written computer programme, simulating the mathematical model , can be integrated with any design routine of high-starting torque squirrel cage induction motors. It calculates the temperature behaviour at a group of successive locations on the bar-depth in addition to the temperature distribution along the bar-depth at different instants during starting towards steady-state. Effect of wedge shaping on the attained maximum and operating temperatures had been studied ; especially after frequent restarts under rated or different load-ratios. The analysis of the computed results forms a knowledge-base which supports the choice decision about the wedge-shape, operational limits and thermal information required for protection systems.

1. INTRODUCTION :

High starting torque squirrel-cage induction motors are the most widely used industrial machines due to their well known benefits compared with other drives. One important design aspect of these motors is the rotor cage thermal behaviour. It must be properly estimated in order to improve the motor reliability. Also, rotor-cage temperature information has become useful in adjusting the protection systems of large motors, and in the design of inverter driven variable speed small

and medium sized motors.

Mathematical efforts have been done to compute the time variation of temperature at several locations on the rotor circuit [1-3]. Part of these efforts is based on the thermal network concept. The other part makes use of the Finite Element (FE) analysis method.

According to the designer point of view, the FE-method is coupled with some difficulties such as the level of discretization and the conditions to be examined [2]. Actually the thermal network concept is more convenient for electrical engineer where the corresponding analysis is very easy to be integrated with the machine design routines. The only drawback of the method based on this concept is the need to build the thermal equation system by hand [4]. Therefore, it is a tedious work ; especially when different operating conditions are to be studied.

In this paper the mentioned drawback of the thermal network method is removed by applying the Network Topological analysis. A relevant computer routine has been written to take over the whole building process of the thermal equations, which are built in form of a state equation ;

$$\dot{\theta}(t) = A \cdot \theta(t) + B(t)$$

The order of this equation depends on the number of observation points that is equal to the number of sub-sections (N) ; into which the rotor-bar cross-sectional area is divided, Fig.(1) . The matrix A is function of the reduced thermal conductance matrix G of the proposed thermal network. The vector B(t) includes the heat sources applied to the nodes. These sources are mainly the copper losses produced within the subsections, where iron losses can be neglected as discussed later. Solving the constructed equation system, the temperature behaviour at the different locations of observation and the temperature distribution at a given instant along the bar-depth can be calculated under the following types of operation :

1. Continuous operation: the motor may start and accelerate to steady speed under a given load.
2. Succesive restart operation : the motor may restart and accelerate each time to steady-speed in successive manner without stop under rated or cyclic load.

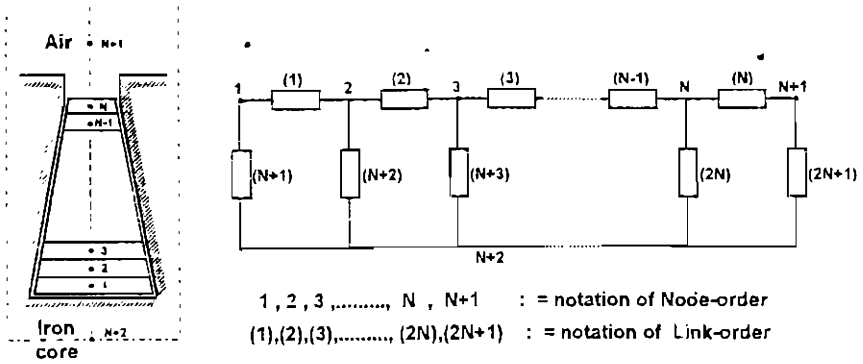

Fig. (1) : Cross-Sectional Subdivisions of the Bar and the Equivalent Thermal Network.

2. MATHEMATICAL FORMULATION :

As mentioned above, the proposed mathematical model is based on the thermal network concept. Therefore, a thermal pattern of the rotor-bar must be suggested in order to build the corresponding thermal network. The mathematical formulation passes through two phases. In the first phase, the thermal network is constructed to simulate the heat transfer within the thermal pettern of the bar. In the second phase, the topologically built first order differential equation system is solved under the requested operating condition to get the corresponding temperature behaviour.

2.1. Thermal Pattern and Equivalent Thermal Network :

Although the proposed mathematical model can handle with any conductor shape ; the wedge type is chosen for sake of explanation. A repetitive thermal pattern around the air-gap has been chosen with the following borders :

- Circumference wise ; one slot pitch about centre-line.
- Axial wise ; one iron packet.

In this pattern the cross-sectional area of the bar can be divided into N fictitious subsections. Each subsection will be represented by one node in the equivalent thermal network, Fig.(1). Dimensionally, a node representing a subsection is assumed to be located at its centre of gravity. It is also assumed that the copper loss consumed in each

subsection is the source of heat produced in this section, and is located attached to the corresponding node. Further, the thermal network has two additional nodes ; the iron and the coolant nodes.

The coolant node (N+1) simulates the surrounding coolant in the air-gap and the internal ventilating ducts. The iron node (N+2) simulates the laminated iron core portion belonging to the thermal pattern. In the presented analysis the eddy current and hysteresis losses (iron losses) are assumed to be negligible. This assumption is taken due to :

- The rotor frequency during the run-up period is decreasing.
- The thermal resistances between the slot and bar are too large.

Therefore, the main contributor to the heating of the rotor is the bar copper losses (I^2R), either under starting or running conditions. According to the above assumption about the iron losses, it is expected that the iron temperature will be approximately constant. Dimensionally, the iron node is taken as the plane going through the axes of the two neighboring teeth and the level located at one third the core depth under the slot bottom as well as the iron surfaces facing the coolant ducts. The heat transfer paths within the thermal pattern, and in turn between the suggested nodes of the equivalent thermal network, can be described as follows :

- Conductive transfer from subsection node to the other , i.e., within the bar itself. Each of the serial branches (1), (2), .. , (N-1), includes the thermal conductance of the corresponding path.
- Conductive transfer from each subsection node to the iron node . Each of the shunt branches (N+1) ,(N+2) ,.... ,(2N) includes the equivalent thermal conductance of two or three parallel paths.
- Convective transfer from the last subsections node to the coolant node. The serial branch (N) includes the corresponding thermal conductance.
- Convective transfer from iron node to the coolant node. The shunt branch (2N+1) includes the corresponding thermal conductance.

The number of nodes and branches of the completed thermal network depends on the number of subsections :

number of nodes $N_n = N + 2$

number of branches $N_b = 2N + 1$

The thermal conductance included in each branch is calculated according to the relevant rules in the heat transfer theory.

2.2. Heat Balance and Thermal Equations :

Thermal equations of the configured equivalent thermal network can be written on the basis of the instantaneous heat balance at each node. Each of these equations has the following form :

$$\Sigma q_{i\nu} - \Sigma q_{o\nu} + d_\nu = (m \cdot C \cdot \dot{\theta})_\nu \qquad (1)$$

where ;

ν := node order 1,2,3,...,N+2

$\Sigma q_{i\nu}$:= sum of rate of change of heat transferred towards the node.

$\Sigma q_{o\nu}$:= sum of rate of change of heat transferred outwards the node.

d_ν := rate of change of heat produced at the node ; equal to either the copper loss or iron loss.

C := specific heat.

m = mass related to a node.

$\dot{\theta}$:= temperature rate of change at the node = $d\theta/dt$.

The sum of heat transferred towards and outwards of the νth node depends on the temperatures of the neighbouring nodes and the temperature level of that node. It depends also on the thermal conductances of the attached branches.

Assuming that $q_\nu = \Sigma q_i - \Sigma q_o$ then :

$$\begin{aligned}
q_1 &= g_{1,2}\cdot(\theta_1 - \theta_2) + g_{1,N+2}\cdot(\theta_1 - \theta_{N+2}) \\
q_2 &= -g_{1,2}\cdot(\theta_1 - \theta_2) + g_{2,3}\cdot(\theta_2 - \theta_3) + g_{2,N+2}\cdot(\theta_2 - \theta_{N+2}) \\
q_3 &= -g_{2,3}\cdot(\theta_2 - \theta_3) + g_{3,4}\cdot(\theta_3 - \theta_4) + g_{3,N+2}\cdot(\theta_3 - \theta_{N+2}) \\
&\vdots \\
q_N &= -g_{N-1,N}\cdot(\theta_{N-1,N} - \theta_N) + g_{N,N+1}\cdot(\theta_N - \theta_{N+1}) \\
&\qquad + g_{N,N+2}\cdot(\theta_N - \theta_{N+2}) \\
q_{N+1} &= -g_{N,N+1}\cdot(\theta_N - \theta_{N+1}) + g_{N+1,N+2}\cdot(\theta_{N+1} - \theta_{N+2}) \\
q_{N+2} &= -g_{1,N+2}\cdot(\theta_1 - \theta_{N+2}) - g_{2,N+2}\cdot(\theta_2 - \theta_{N+2}) \\
&\qquad - g_{N,N+2}\cdot(\theta_N - \theta_{N+2}) - \ldots - g_{N+1,N+2}\cdot(\theta_{N+1} - \theta_{N+2})
\end{aligned} \qquad (2)$$

Where $g_{\nu,\mu}$ is the equivalent thermal conductance of the paths forming the branch linking between the node ν and the node μ.

The above notation can be rewritten in matrix form as :

$$\underline{q} = \underline{G} \cdot \underline{\vartheta}(t) \qquad (3)$$

Where ;

$\underline{G}$:= reducible thermal conductance matrix , [N+2,N+2]

$\underline{\vartheta}$:= reducible vector of node temperatures, [N+2] .

By duality, the $\underline{G}$ matrix has the same structure as that of the reducible electric conductance matrix, known in the "Nodal Analysis" of electric networks. With help of notation (3) , the reducible system of first order differential equations describing the temperature behaviour can be written as :

$$\dot{\underline{\vartheta}}(t) = \underline{A} \cdot \underline{\vartheta}(t) + \underline{B}(t) \qquad (4)$$

where ;

$\underline{A}$:= constant matrix , [N+2,N+2] = $\underline{K}^{-1} \cdot \underline{G}$ (5-1)

$\underline{B}(t)$:= $\underline{K}^{-1} \cdot \underline{D}(t)$ (5-2)

D(t) := reducible colcumn matrix of produced heat attached to nodes , [N+2] (5-3)

The matrix $\underline{K}$ is a diagonal matrix, [N+2,N+2], in which each diagonal element is :-

$$(\underline{K})_{\nu,\nu} = m_{\nu} \cdot C_{\nu} \qquad (5-4)$$

and

$$(\underline{K}^{-1})_{\nu,\nu} = 1/(m_{\nu} \cdot C_{\nu}) \qquad (5-5)$$

The equation system (4) is a dependent one and must be reduced by an equation. As discussed before, the temperature of iron node can be assumed constant. Accordingly, the iron node is taken as reference node having a reference temperature ϑ_{ref} . The corresponding equation is eliminated from the equation system (4) to become :

$$\dot{\vartheta}(t) = A.\vartheta(t) + B(t) \qquad (6)$$

This equation gives the reduced independent equation system. Its

solution yields the behaviour of the temperature-rise at the different nodes ; except the iron node :

$$[\Delta\theta] = \theta(t)$$

Thus, the vector of the temperature behaviour at the different nodes will be :

$$[THETA] = \theta(t) + [\theta_{ref}] \qquad (7)$$

The equation system (6) has the form of a state equation with the solution :

$$\theta(t) = e^{AT}.\theta(0) + A^{-1}.B(t) \qquad (8)$$

This solution is composed of two solutions:

(a) The homogeneous or transient solution

$$[\theta]_H = e^{At} . \theta(0) \qquad (9\text{-}1)$$

(b) The particular integral or steady-state solution

$$[\theta]_{st} = A^{-1}.B(t) = A^{-1}.K^{-1}.D(t) \qquad (9\text{-}2)$$

where :

e^{AT} := the transition matrix

$$= I + A . \frac{\tau}{1!} + A^2 . \frac{\tau^2}{2!} + A^3 . \frac{\tau^3}{3!} + \ldots \qquad (9\text{-}3)$$

τ := time interval

$\theta(0)$:= initial vector of temperatures for next interval

$$= [\theta]_H + [\theta]_{st} \qquad (9\text{-}4)$$

In addition to the above solution, numerical methods can be applied. Whatever is the method of solution, the calculation of D(t) is required from interval to interval with $t_{\nu+1} = t_\nu + \tau$. This reduced vector has mainly the copper losses consumed in to the subsection nodes.

2.3. Copper-Loss Calculation :

A deep-bar cage is designed to have large resistance at stator frequency , instant of starting , employing the influence of skin effect. Due to large rotor resistance, high starting torque can be

exerted. Beginning at this instant, the bar-current is forced to flow within the upper portion of the bar. Accordingly, it can be assumed that the bar-resistance and the slot leakage reactance are dependable during the period of run-up on the penetration depths h_{pr} and h_{pl} , respectively [8,9] .

$$h_{pr} = 0.010/\sqrt{s \cdot \frac{f}{50} \cdot \frac{g_c(\theta)}{50}} \quad , \quad m \qquad (10\text{-}1)$$

$$h_{pl} = 0.015/\sqrt{s \cdot \frac{f}{50} \cdot \frac{g_c(\theta)}{50}} \quad , \quad m \qquad (10\text{-}2)$$

Where ;

s := slip , f := supply frequency , and

$g_c(\theta)$:= copper temperature dependent conductivity.

As the rotor accelerates, the rotor frequency decreases ($f_2 = sf$) and both h_{pr} and h_{pl} become greater. Finally, each will be equal to the bar-depth and the bar current will be distributed over the whole bar cross-section. Under running condition the rotor resistance has its nominal value reducing thereby the rotor copper loss.

It is seen that the bar current density , j(t) , will be time varying from point to point along the bar-depth [7].

$$j(t) = \frac{I_m(t)}{b} \left[\sum_{n=1}^{n=\infty} \left\{ \frac{2(n.\pi.k)^2.\omega(-1)^n}{h^3.(\omega^2+(n\pi k/h)^4)} \cdot e^{-(n\pi k/h)^2.t} \cdot \cos(2\pi y/h) \right\} - \right.$$

$$\left. - \sqrt{\frac{(\cosh(y/AA).\cos(y/AA))^2 + (\sinh(y/AA).\sin(y/AA))^2}{(\sinh(h/AA).\cos(h/AA))^2 + (\cosh(h/AA).\sin(h/AA))^2}} \right.$$

$$\left. \cdot \frac{\sqrt{2}}{AA} \cdot \sin(\omega t + \alpha_2) \right] \qquad (11)$$

where ;

$I_m(t)$:= maximum sinusoidal time varying bar current ,

h and b' := equivalent height and width of the bar ; respectively [9]

y := depth of the subsection node ; measured from the upper conductor surface.

α := ratio of bar width to slot width at any depth = 1.0

$$K^2 := \alpha.\rho/\mu = \rho/\mu \qquad (12\text{-}1)$$

ρ and μ := resistivity and permeability of conductor material ; respectively.

$$\alpha_2 = \frac{\pi}{4} + \tan^{-1}[\tanh(y/AA).\tan(y/AA)] - \tan^{-1}[\operatorname{cotanh}(h/AA).\tan(h/AA)] \qquad (12\text{-}2)$$

$$AA = k \cdot \sqrt{2/\omega} \qquad (12\text{-}3)$$

With help of the above relation, Eq.(11) over the time interval τ , the r.m.s. value of the bar current density , $J(t)$, is calculated to get the copper loss occurring in each subsection :

$$(D(t))_\nu = [p_c(\theta) \cdot G_c \cdot J(t)]_\nu \quad , \quad W \qquad (13)$$

where ;

$\nu = 1,2,3 \ldots\ldots,N$

$p_c(\theta)$:= specific copper loss

$$= \frac{1000}{\gamma(g_c(\theta))_\nu} \quad , \quad W/Kg \qquad (14\text{-}1)$$

γ := copper density = 8950 , Kg/m^3

$$(g_c(\theta))_\nu = g_c(20) \cdot \frac{255}{235 + \theta_\nu} \qquad (14\text{-}2)$$

$g_c(20) = 57.$, $m/mm^2.\Omega$

2.4. Calculation of $I_m(t)$:

The maximum sinusoidal time varying rotor-bar current is calculated assuming a conventional equivalent-circuit per phase ; but with slip varying rotor parameters r_2 and x_2. The bar resistance, and then r_2 is calculated each time interval taking into consideration the resistance penetration depth, h_{pr} , and the effect of the average bar-temperature. Similarly, the rotor specific permeance, and then x_2 is calculated each

time interval taking into consideration the inductance penetration depth, h_{pi} . Thereby the rotor resistance and leakage inductance are renewed each time interval ; until skin-effect loses its influences. Here, $h_{pr} = h_{pi}$ = the bar depth.

3. COMPUTER SIMULATION :

An essential feature of the suggested mathematical model is the ability of applying the topological analysis [5,8]. The main computer programme includes two adequate subroutines **GRAPH** and **INCMAT** to dail with the topological formulation of a proposed thermal network. According to the given number of subsections N , the subroutine **GRAPH** follows the predescribed thermal network configuration , Fig. (1) , to construct the list of branches : LINKS [4N+2,3]. In this list, each branch is represented twice in the forward and backward directions of heat-flow. Each time, the branch is defined by its order, start-node, and end-node. With help of LINKS , the subroutine INCMAT builds the reducible incident matrix INC [N+2,2N+1] . This matrix reflects the nodal configuration of network. The rows and columns are denoted by the node and branch orders :

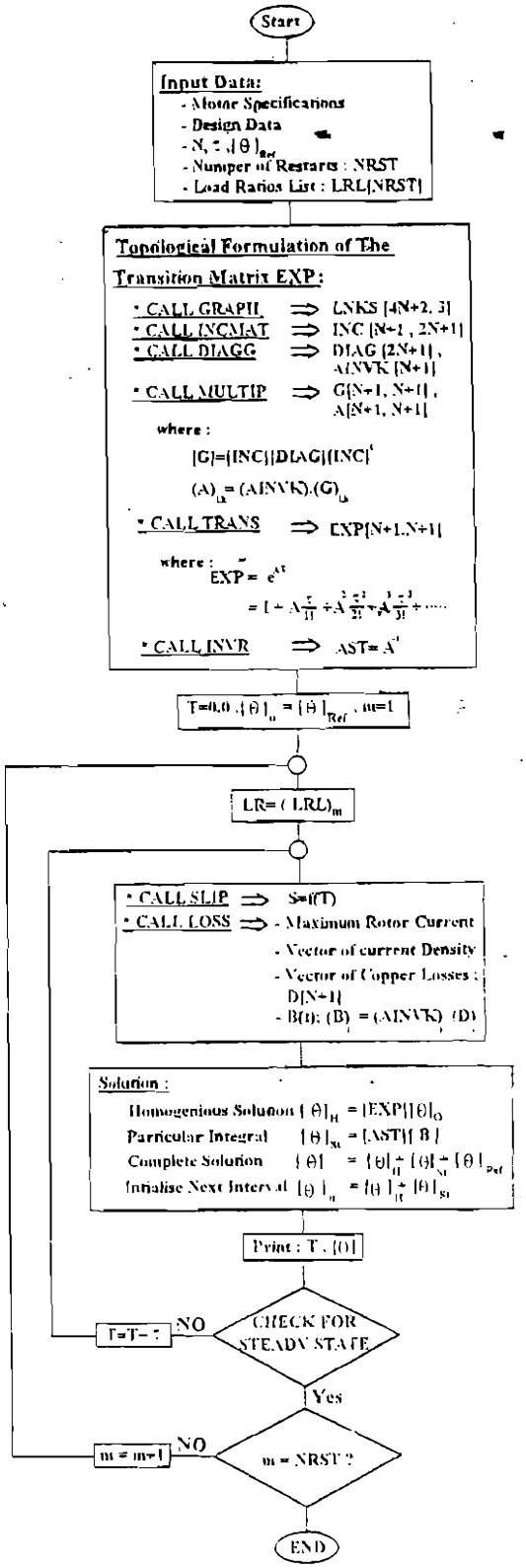

Fig. (2) : Flow Chart

(1,2,3, ...,N+2) and ((1),(2),(3),...,(2N+1)) ; respectively.
Any element $(INC)_{n,m}$ may be (+1) , (-1) or(0). As each branch links between two nodes, the sum of elements in each coloumn of INC must be zero : only (+1) and (-1) in correspondence with the start and end nodes ; respectively. Rest of the coloumn elements are zeroes. The reduced INC-matrix [N+1,2N+1] is obtained by eliminating the last row corresponding to the iron node N+2.
The subroutine DIAGG is concerned with the calculations of the matrices DIAG and AINVK . Each is a constant diagonal matrix stored in form of one coloumn list. The matrix AINVK [N+1] is built according to the relation (5-5). The matrix DIAG [2N+1] contains the equivalent thermal conductances of the network branches;

Serial branches : (1),(2),(3),...,(N)
and Shunt branches : (N+1),(N+2),...,(2N+1).

A serial-branch conductance simulates one thermal path between two successive nodes in the node group 1,2,3,...,N+1. A shunt branch conductance simulates two or three thermal paths in parallel existing between each of the successive nodes and the reference node N+2. With the above topologically formulated matrices, the conductance matrix G , and the constant matrix A and its inverse can be built :

$$[G] = [INC][DIAG][INC]^t \qquad (15)$$

$$[A] = [AINVK][G] \qquad (5\text{-}1)$$

Each is reduced and has the dimension [N+1,N+1].
Now, the transition matrix $[EXP] = [e^{AT}]$ can be calculated for the pre-chosen time interval τ according to the expansion given in Eq. (9-3). The above calculations are performed just one time to begin thereafter the repetitive procedure.

The flowchart given in Fig.(2) illustrates the calculation process. Relevant subroutines are written to get the system solution ; interval by interval. Thereby, the temperature behaviour at N locations of observation along the bar-depth can be calculated ; under different operating conditions.

4. RESULTS AND DISCUSSIONS :

The figures (3) through (12) demonstrate the capabilities of the suggested mathematical model and the corresponding computer programme as a helpful tool for calculating the expected temperature behaviour within a cage deep-bar. The specifications of the tested machine are 500 Kw , 6000 V , 50 Hz , 125 (synch.) r.p.m ;

ratio of starting torque : 0.5 ;
ratio of starting current : 3.5 ; and
rotor bar : wedge-type with BETA $b_1/b_2 = 0.5$
: designer cross-sectional dimensions :
upper bar-width , $b_1 = 3.9$ mm
lower bar-width , $b_2 = 7.8$ mm
bar height (or depth) , $H = 24.0$ mm

It follows now some brief discussions about the calculated results.

4.1. Simulation Criterion ; Effect of N :

In order to criticize the simulation degree of heat transfer, the number of subsections N is taken as criterion. During this criterion, the ratio of the upper bar-width to lower bar width is held constant at the designer value; i.e., BETA = 0.5 . Figure (3) shows the temperature behaviours during the run-up period towards the rated full load speed ; for N = 1,3,5,7, and 9 . Odd numbers are taken; to have the node corresponding to the middle section at the same location for all N. It is also seen that each node location (or subsection) has an individual temperature behaviour. During the run-up period , about 20 sec. , increases each behaviour to reach a maximum value within 5 seconds. It is seen that the upper section has the highest behaviour. As steady speed is reached, begin the different locations to attain the same steady state temperature. The comparison between the temperature behaviours at the middle sections , Fig.(4) , dictates that the number of subsections must be taken not less than seven (N.NLT.7) . Figure (4) gives also a comparison of the corresponding behaviours of current densities. The evident identity is expected where the current density does not depend on the number of subsections.

4.2. Effect of The Ratio BETA :

One of the design aspects that must be carefully studied is the effect of the ratio BETA on the temperature behaviour and temperature

distribution along the bar-depth ; Fig. (5) to (9). This ratio has also its effects on starting and maximum torques ;i.e., the torque/slip characteristic. Therefore, design modifications have been done to get for each value of BETA the proper bar dimensions H and b_z , Fig.(13). These dimensions ensure that the motor will follow ,to great extent, the same Torque/Slip characteristic ; irrespective of BETA. The temperature behaviour during run-up period toward the rated full load speed has been calculated for different values of BETA ; having the same number of subsections (N=7). Figure (7) shows these behaviours. It is evident that the ratio BETA has a remarkable effect on both the attained maximum and steady-state temperatures. Although Beta = 1.0 results in lowest temperature behaviour Figures (5,6,7) ; it is recommended to take BETA within 0.3 to 0.7 . In this range, optimum torque and temperature behaviours are ensured. Regarding the temperature distribution along the bar depth, Figures (8.9) , it is seen that the upper section has the highest temperature for all values of BETA ; except BETA = 0.1 .

4.3. Effect of Operating Conditions :

The effect of operation conditions on the temperature behaviour is seen in Figures (10 ,11 , and 12). Here, proper BETA and nunber of subsections are taken, BETA = 0.5 and N = 7 . To start the motor under a given load and run continuously under this load ; it is seen in Fig. (10) that the temperature behaviour is the same during the run-up period. Only steady state temperature is affected to become smaller with smaller loads. This behaviour is expected as long as the motor is not locked by load during the run-up period.

Successive restarts, without stop under rated load or different load cycles, have a great effect on the attained transient and steady state temperatures Figs. (11) , (12). Therefore, loading cycles without pauses must be carefully configured in order to prevent faulty rotors.

5. CONCLUSIONS :

In this paper a special computer programme has been written to analyse thermally the deep bar squirrel cage rotors under different operating conditions. The presented mathematical model is based on the equivalent thermal network concept which is more convenient for

electric machine designers. An essential feature of this model is its ability of applying the topological network analysis. Further more, the model takes into consideration both the influence of skin effect on the rotor current , as well as the effect of temperature on the bar resistance and current density.

Accordingly, the programme is able to be integrated with design routines concerned with the design of high starting torque squirrel cage induction motors. Thereby the temperature behaviour at defined locations of observation along the bar-depth can be estimated to a reasonable degree of accuracy. Actually, the number of these locations must be reasonable , not less than seven ; in order to reduce the number of equations.

The demonstrated results show the capability of the programme to study the effects of design , thermal , and operating aspects on the bar temperature behaviour.

REFERENCES :

[1] Griffith J.W. , McCoy R.M. ,Sharma D.K. ,"Induction Motor Squirrel Cage Rotor Winding Thermal Analysis", IEEE Transactions on Energy Conversion , Vol.EC-1, No. 3. , pp. 22-25 .September 1986.

[2] Siyambalapitiya D.J.T., McLaren P.G., Tavner P.J. ,"Transient Thermal Characteristics of Induction Motor Rotor Cage" , IEEE Transactions on Energy Conversion , Vol. 3, No. 4, pp. 849-852, December 1988.

[3] Garg V.K. , Raymond J.M. ,"Magneto-Thermal Analysis of Canned Induction Motor" , IEEE Transactions on Energy Conversion , Vol. 5, No. 1 , pp. 110-114 , March 1990 .

[4] Gaber A.Z.A ,"Temperature Rise in Deep-Bar Induction Motor During Starting" , M.Sc. Thesis Submitted to Department of Electrical Power and Machines , Mansoura University , El-Mansoura 1983.

[5] Byerly R.T. , Long R.W. , King C.W. ,"Logic for Applying Topological Methods to Electric Networks , AIEE Transactions on Communication and Electronics 77 , H 11 , pp.657-667 , 1958.

[6] Reed M.B. , Seshu S. ,"Linear Graphs and Electrical Networks" , Addison-Wesley Publishing , 1961.

[7] Verma S.P., Abo-Shady S.E. ,"Method of Calculation of Transient Skin Effect in Conductors Embeded in Slots for Cage Windings" IEEE Transactions, Vol. PAS-99 , No.6 , Nov./Dec. 1980, pp.2318-2326.

[8] Vickers H.,"The Induction Motor: Theory, Design, and Application", 2. nd Edition , LONDON SIR ISAAC PITMAN & SONS, LTD. , 1953.

[9] Nürnberg W.,"Die Asynchronmaschine", 2. nd Edition,Springer-Verlag Berlin/Gottingen/Heidelberg , 1963.

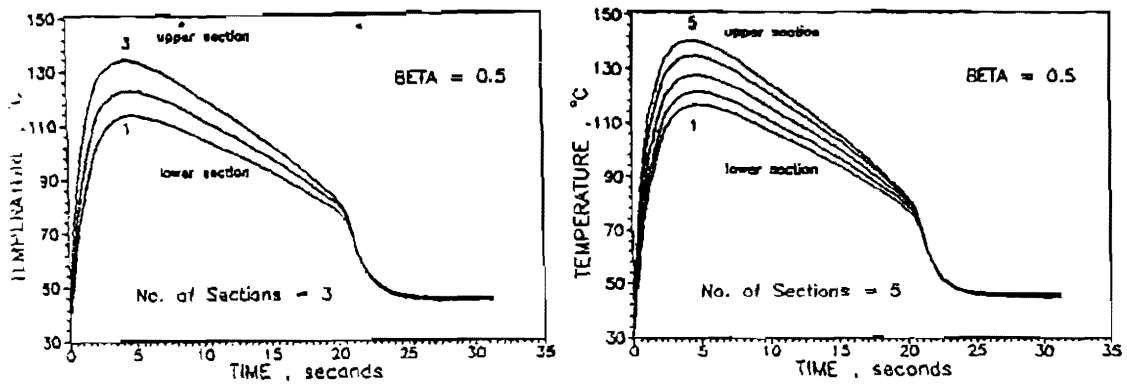

Fig. (3) : Effect of number of Subsections (N) on the temperature behaviour along the bar-depth; Beta = 0.5 .

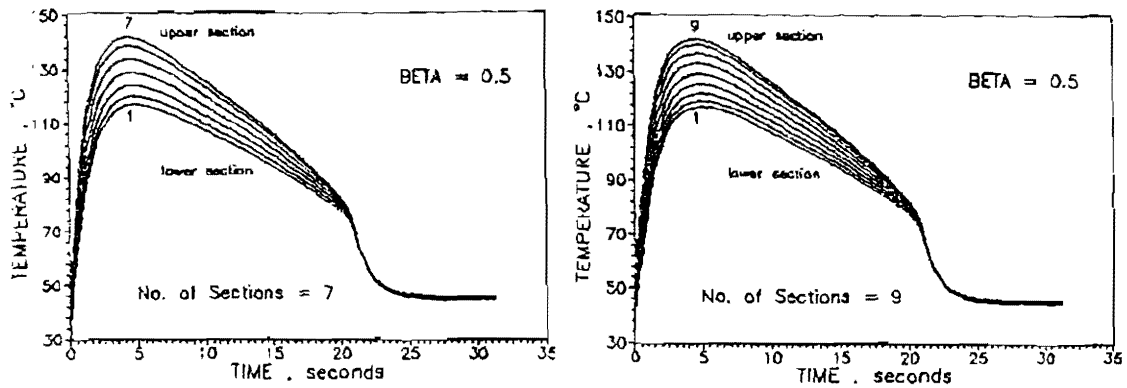

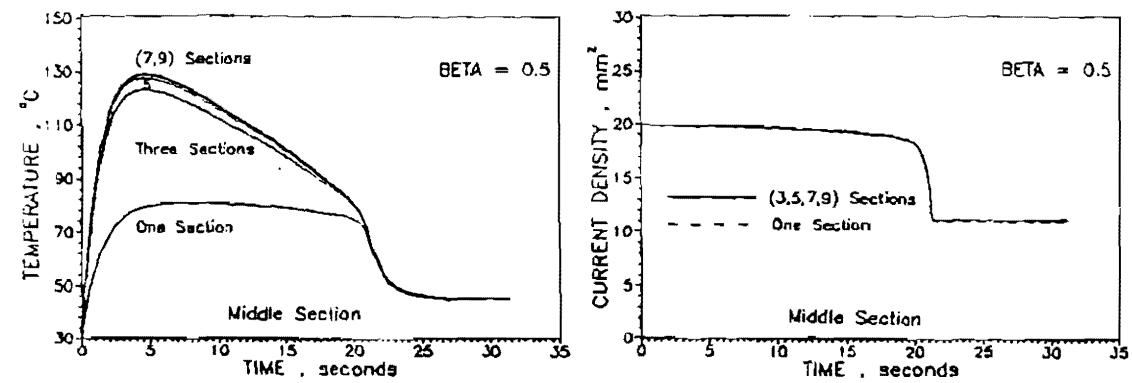

Fig. (4) : Comparison between the temperature behaviours in the middle Subsection for different N, Beta = 0.5, and the corresponding baheviour of current density.

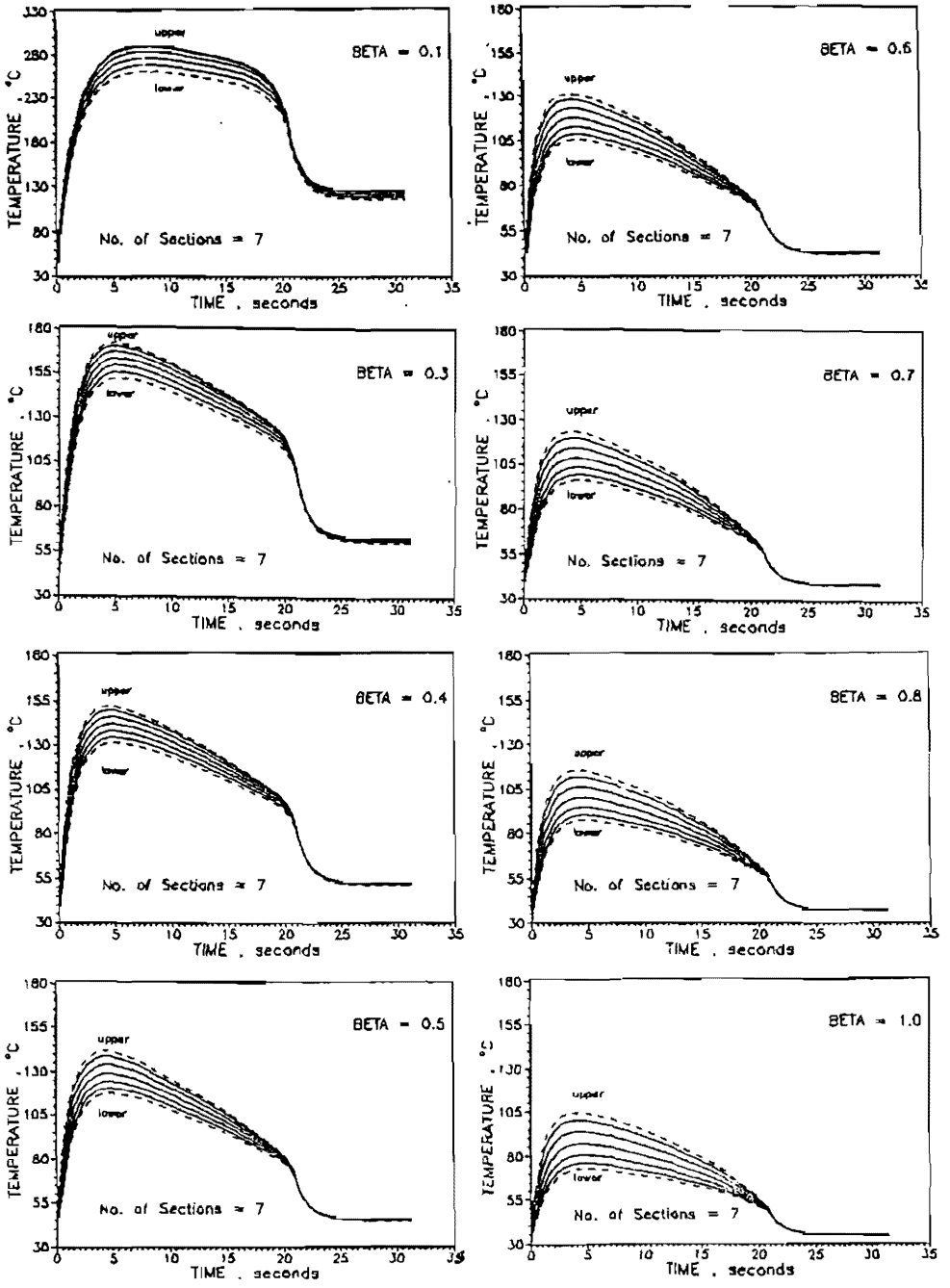

Fig. (5) : Effect of Beta on the temperature beheviour along the bar-depth; same proper number of Subsections (N=7).

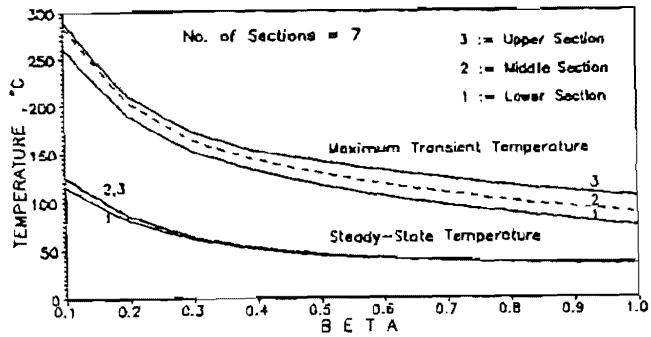

Fig. (6) : Effect of Beta on maximum, transient and steady-state temperatures.

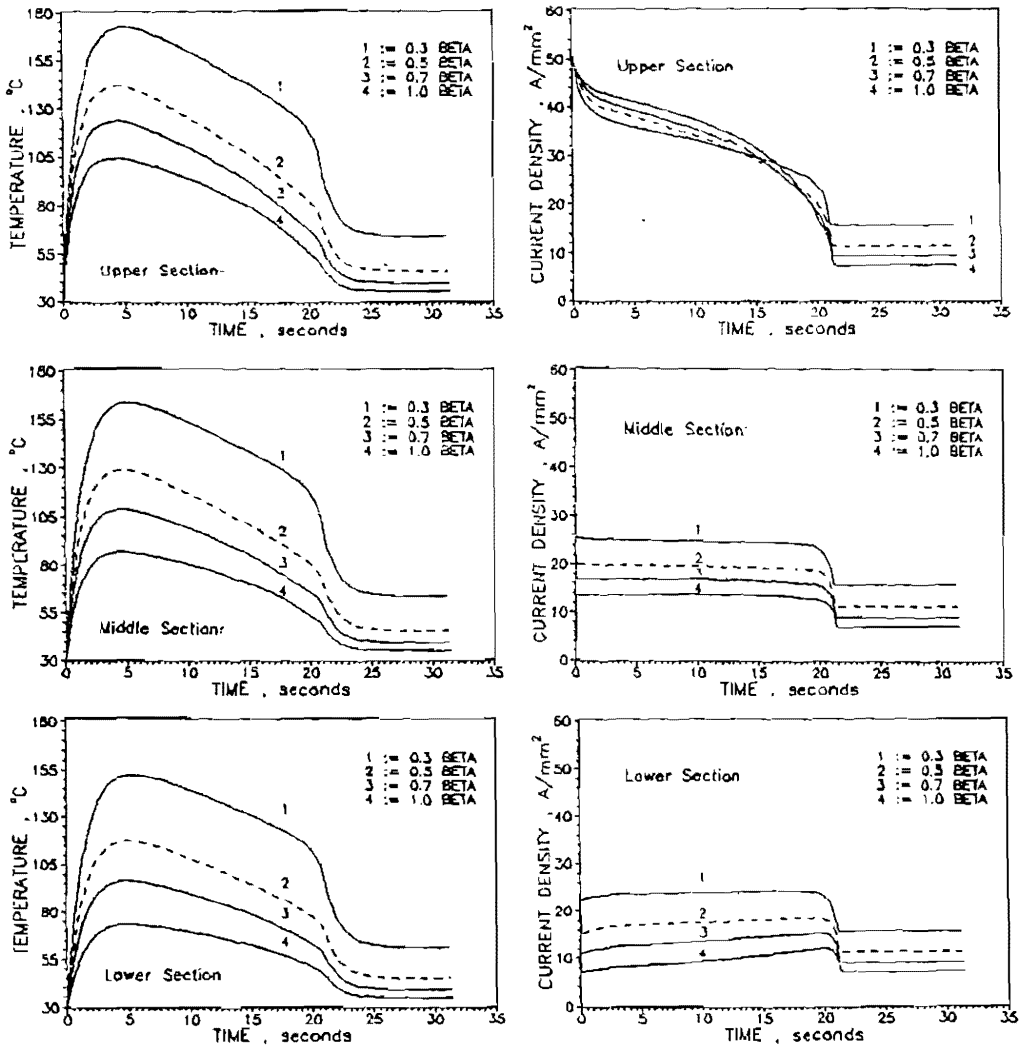

Fig. (7) : Effect of Beta on the temperature behaviour at three salient locations along the bar-depth (N=7), and the corrosponding behaviour of

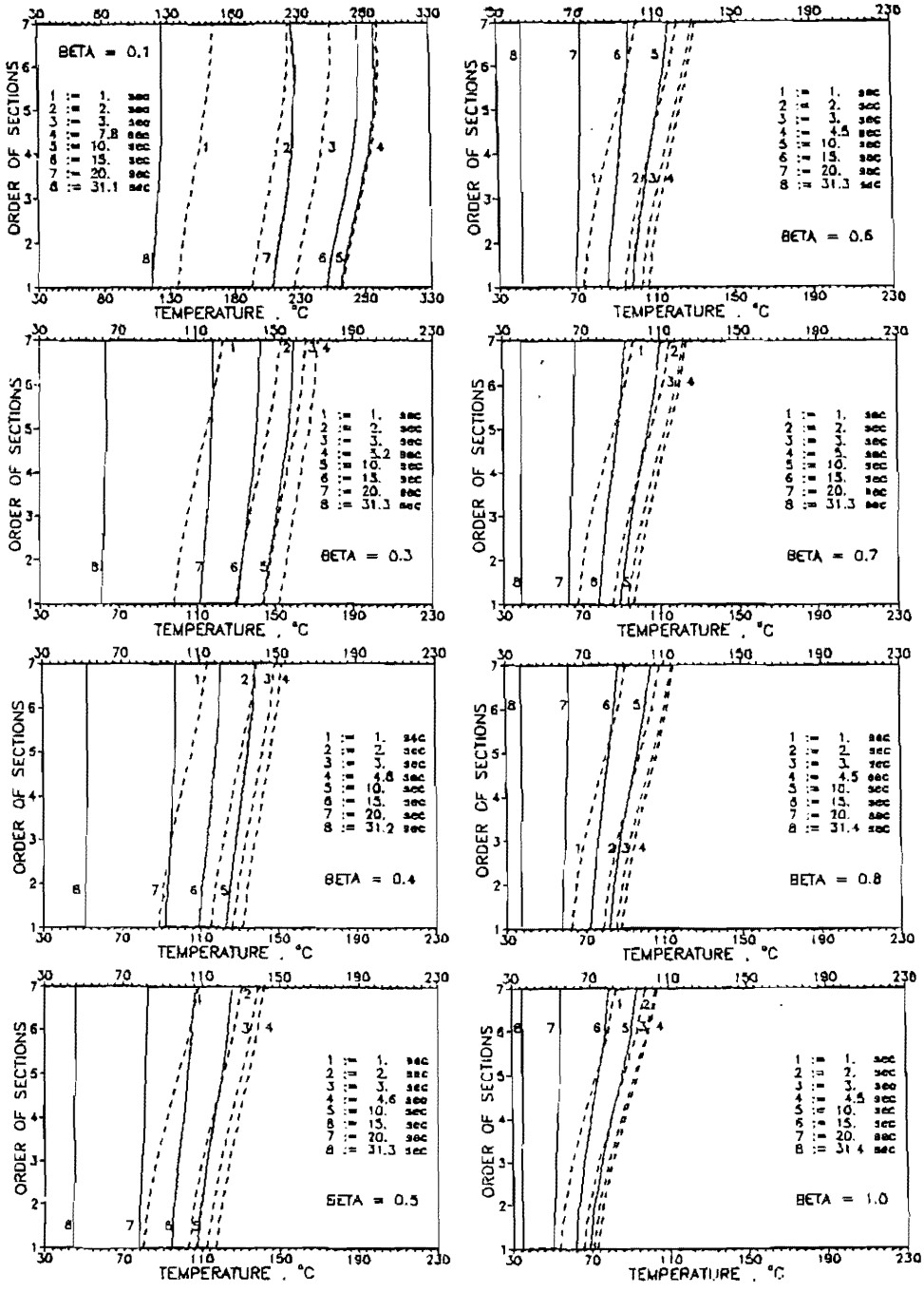

Fig. (8) : A comparison of temperature distribution along the bar-depth for different Beta during the run-up period.

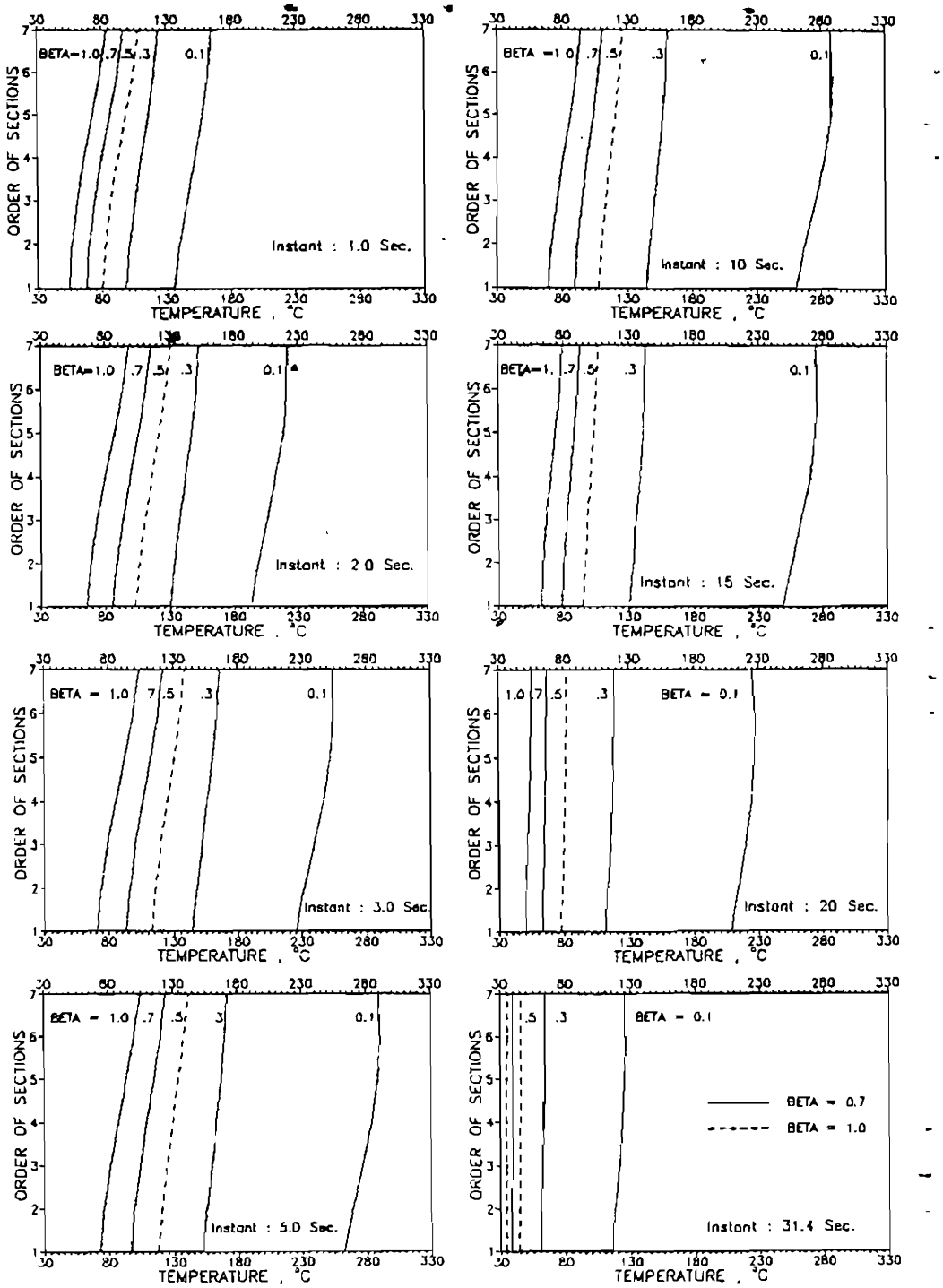

Fig. (9) : Effect of Beta on the temperature - distribution along the bar-depth at given instant during the run-up period. (N=7).

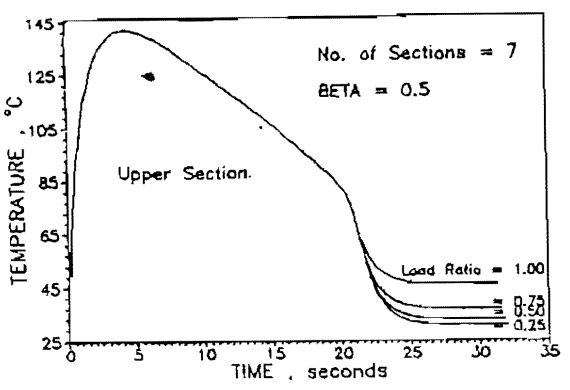

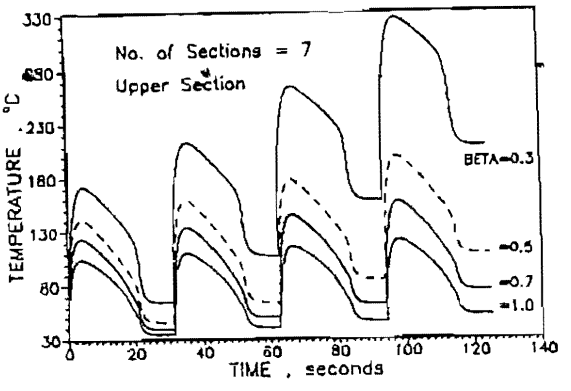

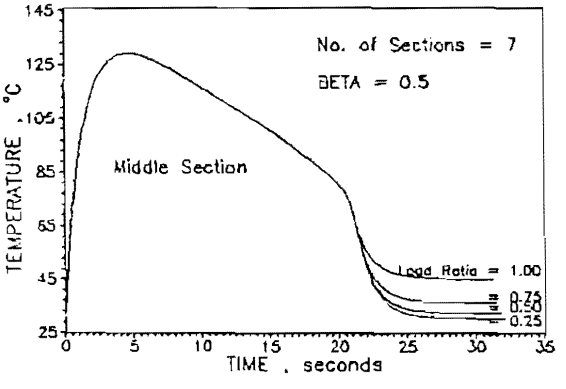

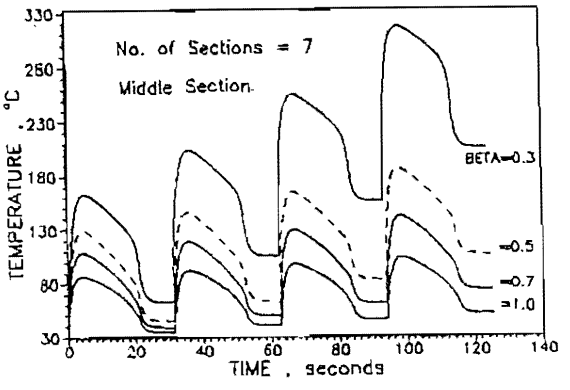

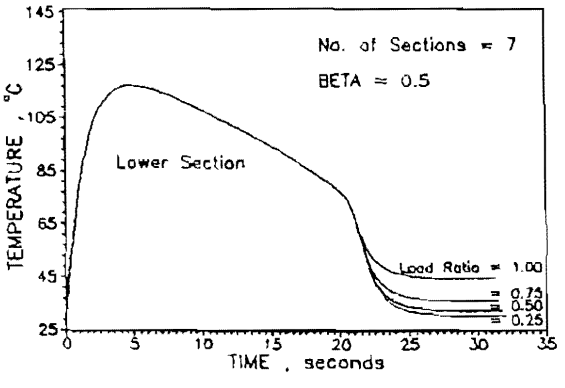

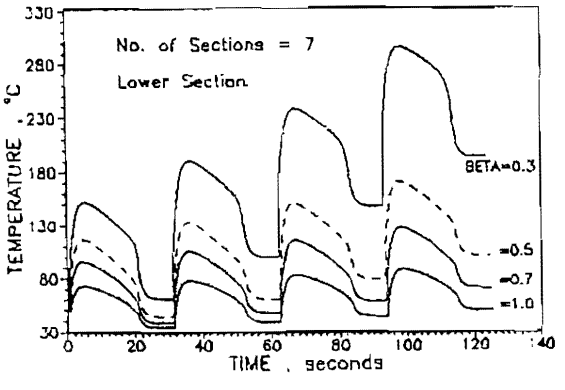

Fig. (10) : Effect of driven load on temperature behaviour.

Fig. (11) : Effect of Beta on temperature behaviour under successive restarts with rated load.

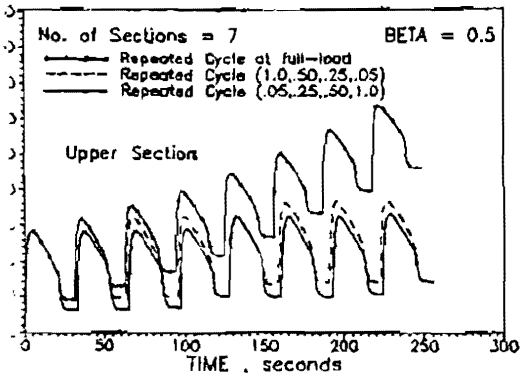

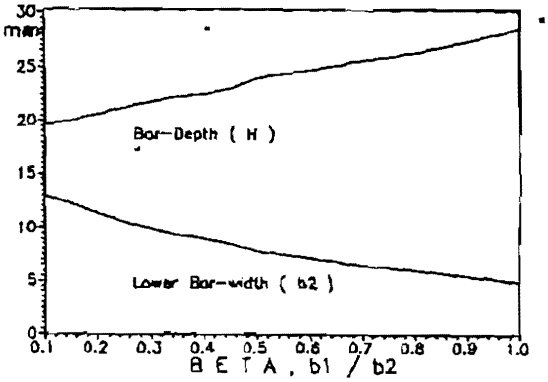

(a)

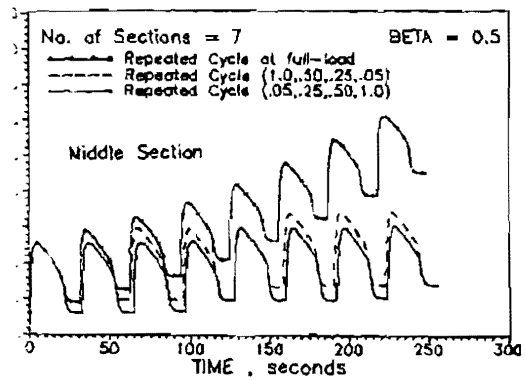

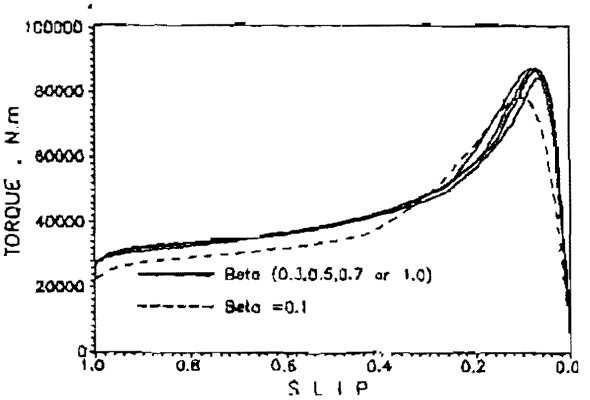

(b)

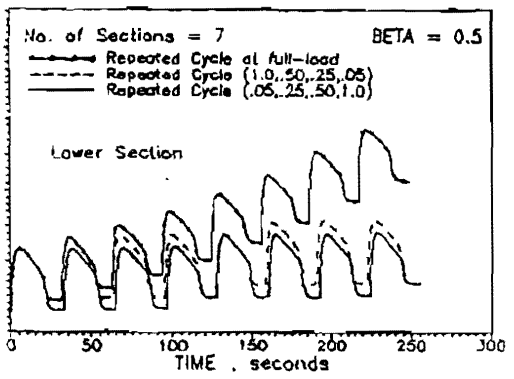

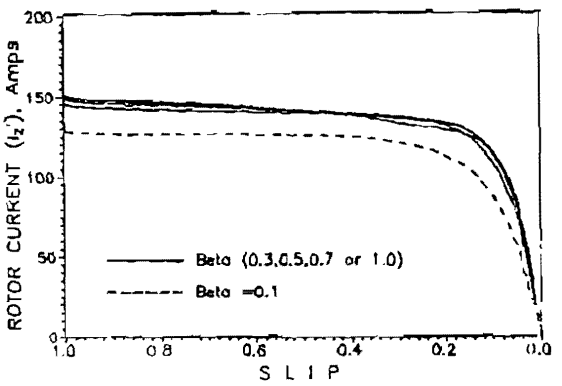

(c)

Fig. (12) : Temperature behaviours under successive restarts with cyclic load compared with that of rated load

Fig. (13) : Some design aspects.
(a) Bar dimensions / Beta.
(b) Torque / Slip, and
(c) Rotor current / Slip.